Photoisomerization of quinolin-2-yl derivatives of β-tropolone

N. I. Makarova,[a]★ A. V. Metelitsa,[a] S. O. Bezuglyi,[b] Yu. A. Sayapin,[a] V. N. Komissarov,[a] A. G. Starikov,[b] M. S. Korobov,[a] G. S. Borodkin,[a] Z. A. Starikova,[c]★ M. Yu. Antipin,[c] and V. I. Minkin[a,b]

[a]*Institute of Physical and Organic Chemistry, Rostov State University, 194/2 prosp. Stachki, 344090 Rostov-on-Don, Russian Federation. Fax: +7 (863) 243 4667. E-mail: photo@ipoc.rsu.ru*
[b]*Southern Scientific Center, Russian Academy of Sciences, 41 ul. Chekhova, 344006 Rostov-on-Don, Russian Federation. E-mail: andr@ipoc.rsu.ru*
[c]*A. N. Nesmeyanov Institute of Organoelement Compounds, Russian Academy of Sciences, 28 ul. Vavilova, 119991 Moscow, Russian Federation. Fax: +7 (495) 135 5085. E-mail: star@xray.ineos.ac.ru*

Photolysis of hexane solutions of quinolin-2-yl-β-tropolones is accompanied by the photoinduced proton transfer O—H...N → O...H—N followed by the disrotatory electrocyclic rearrangement giving rise to 3-(1*H*-quinolin-2-ylidene)bicyclo[3.2.0]hept-6-ene-2,4-dione derivatives. The molecular and crystal structure of one of the compounds isolated preparatively, *viz.*, 1,6-di(*tert*-butyl)-3-(4-chloro-8-methyl-1*H*-quinolin-2-ylidene)bicyclo[3.2.0]hept-6-ene-2,4-dione, was established by X-ray diffraction. The structures, tautomeric transformations, and the structural dynamics of the resulting compounds were studied by *ab initio* quantum chemical methods, absorption and fluorescence spectroscopy, and dynamic NMR spectroscopy.

Key words: β-tropolones, photoisomerization, fluorescence, photoinduced proton transfer, quantum chemical calculations, tautomerism, electrocyclic photorearrangements, X-ray diffraction analysis, bicyclo[3.2.0]hept-6-ene-2,4-diones.

The photoinduced rearrangement of α-tropolones into bicyclo[3.2.0]hepta-3,6-dien-2-one derivatives has been studied in detail,[1—3] whereas data on the analogous photoreaction of β-tropolones were lacking. Recently,[4] we have developed a new procedure for the synthesis of 2-heteryl derivatives of β-tropolones **1** based on the ring expansion in the reaction of 3,5-di(*tert*-butyl)-1,2-benzoquinone with 2-methylquinoline derivatives. In the present study, we carried out photochemical electrocyclization of compounds **1** → **3** and investigated the structures and spectroscopic characteristics of the resulting photoisomers using rearrangement product **3a**, which was isolated preparatively, as an example (Scheme 1).

The long-wavelength region of the electronic absorption spectra of compounds **1a—e** (Table 1) contains an intense structured band with absorption maxima at 383—390 nm (ε = 18200—20500 L mol^{-1} cm^{-1}) and a shoulder at 445 nm (ε = 1500—5000 L mol^{-1} cm^{-1}). At room temperature, solutions of compounds **1a—e** do not show luminescence. However, an intense structured fluorescence band (λ_{max} = 505—530 nm) with an anomalous Stokes shift Δλ = 123—140 nm (Δν ~ 6400—6800 cm) relative to the absorption spectrum is observed at 77 K in hexane. The fluorescence excitation spectra correspond to the long-wavelength absorption bands of compounds **1a—e** (Table 1, Fig. 1).

The above data indicate that excitation of compounds **1a—e** in hexane at 77 K induces the intramolecular proton transfer O—H...N → O...H—N (**1** → *E*-**2**) giving rise to the state S_1 of the emitting NH-structure *E*-**2** (Scheme 1).

Table 1. Fluorescence spectral properties of compounds **1a—e** in hexane

Compound	Absorption λ_{max}/nm ($\varepsilon \cdot 10^{-3}$)*	Fluorescence (excitation) λ_{max}/nm	Stokes shift $\Delta\lambda_{max}$/nm
1a	382 (18.2), 445 sh (2.8)	505 (397)	123
1b	383 (19.0), 445 sh (5.0)	510 (395)	127
1c	383 (19.8), 445 sh (3.0)	510 (395)	127
1d	390 (18.8), 445 sh (2.1)	530 (395)	140
1e	387 (20.5), 445 sh (1.5)	520 (395)	133

* L mol^{-1} cm^{-1}.

Published in Russian in *Izvestiya Akademii Nauk. Seriya Khimicheskaya,* No. 3, pp. 467—474, March, 2006.

Scheme 1

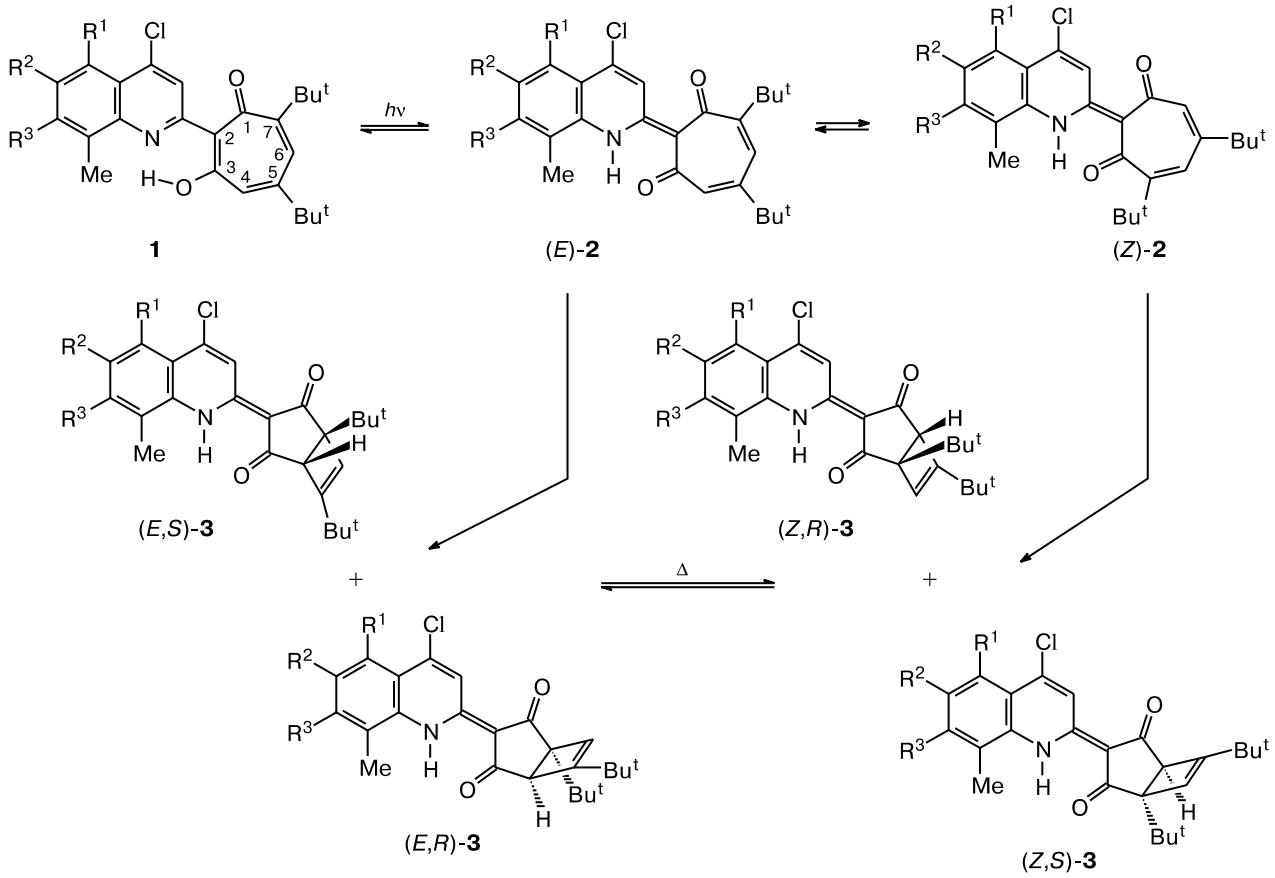

$R^1 = R^2 = R^3 = H$ (**a**); $R^1 = R^2 = H$, $R^3 = Me$ (**b**); $R^1 = R^3 = H$, $R^2 = Me$ (**c**); $R^1 = NO_2$, $R^2 = H$, $R^3 = Me$ (**d**); $R^1 = NO_2$, $R^2 = Me$, $R^3 = H$ (**e**)

The yield of (*E*,*S*)-**3** + (*E*,*R*)-**3** was 40%; (*Z*,*R*)-**3** + (*Z*,*S*)-**3**, 60%.

Irradiation of solutions of compounds **1a—e** in hexane at room temperature in the long-wavelength absorption band (λ_{rad} = 365 nm) leads to a similar irreversible modification of the absorption spectra of all compounds associated with the appearance of a new structured band (λ_{max} = 400—463 nm). The photoinduced changes in the absorption spectrum of compound **1a** are shown in Fig. 2.

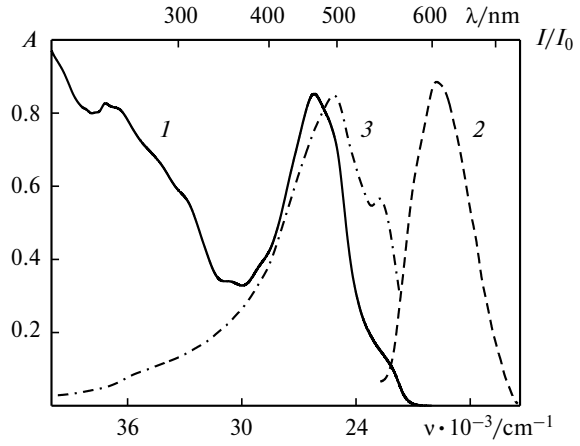

Fig. 1. Absorption spectra (*1*) ($C = 4.68 \cdot 10^{-5}$ mol L^{-1}, T = 293 K), fluorescence spectra (*2*) (λ_{exc} = 370 nm, T = 77 K), and fluorescence excitation spectra (*3*) (λ_{obs} = 510 nm, T = 77 K) of compound **1a** in hexane.

As is evident from the anomalous Stokes shift of the fluorescence spectrum, it is the NH form that is the major one in the excited state, and a suitable diene system exists only in this form. Hence, the photoisomers would be expected to have a bicyclo[3.2.0]hept-6-ene-2,4-dione structure of type **3**. The disrotatory photoelectrocyclization of β-tropolones **1** allowed by the orbital-symmetry rules can occur from the *trans* (*E*-**2**) and *cis* isomers (*Z*-**2**) as a results of the cyclobutene ring closure following two possible pathways (see Scheme 2) to give a mixture of isomers (*E*,*S*)-**3**, (*E*,*R*)-**3** and (*Z*,*R*)-**3**, (*Z*,*S*)-**3**, respectively.

X-ray diffraction study of compound **3a**, which was isolated in 65% yield and prepared by photoisomerization of β-tropolone **1a**, provided unambiguous evidence for this direction of the photoreaction.

The luminescence spectral characteristics of photoproducts **3a—e** are given in Table 2. The quantum yields of photoreaction **1a** → **3a** are $4.2 \cdot 10^{-4}$ and $4.8 \cdot 10^{-4}$ in

Scheme 2

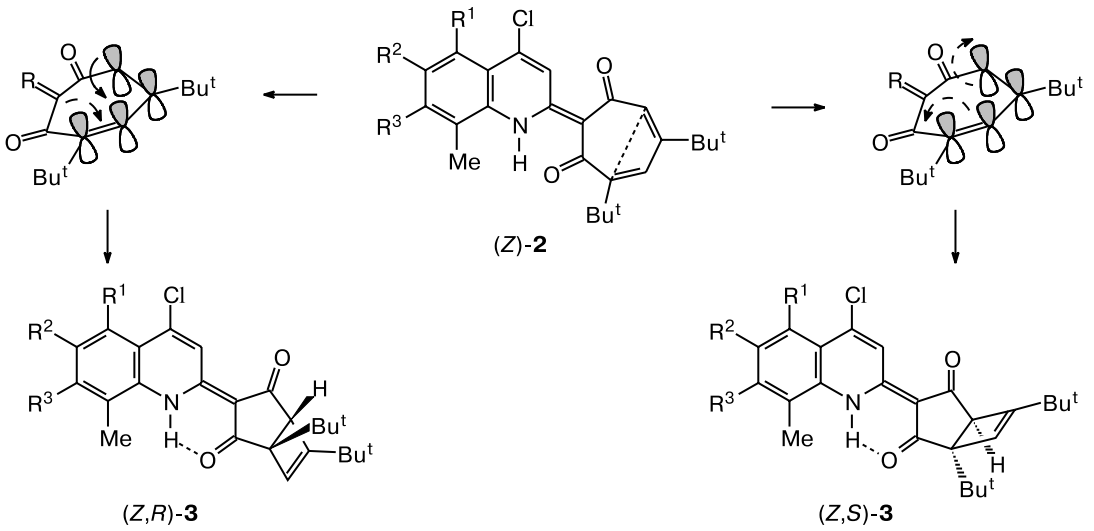

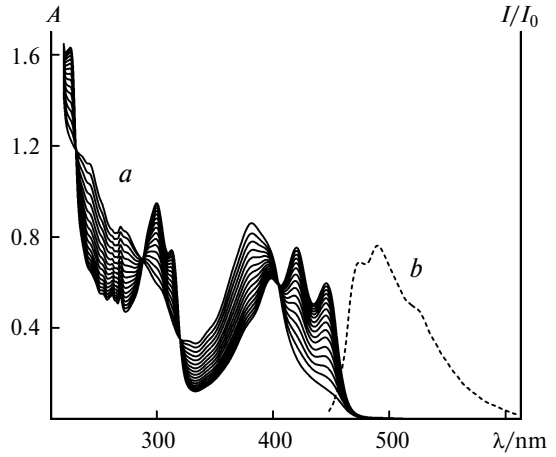

Fig. 2. Photoinduced changes in the electronic absorption spectra (*a*) upon irradiation (λ_{rad} = 365 nm; at 5 min intervals) of a solution of compound **1a** ($C = 4.68 \cdot 10^{-5}$ mol L^{-1}) and the fluorescence spectrum (*b*) of photoproduct **3a** in hexane at $T = 293$ K.

Table 2. Luminescence spectral properties of photoproducts **3a—e** in heptane

Compound	Absorption λ_{max}/nm ($\varepsilon \cdot 10^{-3}$)*	Fluorescence λ_{max}/nm
3a	399 (12.6), 420 (19.5), 446 (16.0)	470, 490, 520 (sh)
3b	401, 422, 448	470, 490, 520 (sh)
3c	400 (12.8), 422 (19.8), 448 (16.2)	470, 495, 520 (sh)
3d	410, 435, 463	490, 520, 550 (sh)
3e	406, 434, 463	490, 515, 550 (sh)

* ε/L mol^{-1} cm^{-1}.

hexane and toluene, respectively. At room temperature, photoisomerization products **3a—e** show intense structured fluorescence at room temperature with two maxima at 470—520 nm and a shoulder at 520—550 nm (Fig. 2, Table 2). The fluorescence excitation spectra of photoproducts **3a—e** are identical to the absorption spectra of these compounds. The fluorescence quantum yields for photoproducts **3a** and **3c** are 0.11 and 0.15 (in toluene), respectively.

Compounds **3a,c** were isolated preparatively. The molecular structure of **3a** was established by X-ray diffraction. The overall view of molecule **3a** is shown in Fig. 3. The main geometric parameters of molecule **3a** are given in Tables 3 and 4.

The crystal structure of 1,6-di(*tert*-butyl)-3-(4-chloro-8-methyl-1*H*-quinolin-2-ylidene)bicyclo[3.2.0]hept-6-ene-2,4-dione (**3a**) contains two crystallographically independent molecules, (*Z*,*R*)-**3a** and (*Z*,*S*)-**3a**, which differ in the orientation of the four-membered ring (and, correspondingly, the orientation of the *tert*-butyl substituents) relative to the planar system composed of the quinoline and cyclopentadione rings. The dihedral angle between the plane of this system (the N(1), O(1), O(2), C(1)—C(13), C(16), and C(17) atoms) and the plane of the four-membered ring (the C(13)—C(16) atoms) is equal in both molecules (61.3°), but the orientation of the four-membered ring relative to the plane of the system in molecule (*Z*,*R*)-**3a** is opposite to that in molecule (*Z*,*S*)-**3a**. The parameters of the intramolecular N—H...O hydrogen bond are equal in both independent molecules (O...H, 1.89 Å; N...O, 2.598 Å; N—H(N)—O, 139°).

The C(1)—C(11), C(1)—N(1), C(11)—C(12), and C(11)—C(17) bond lengths (the average values are 1.401, 1.336, 1.438, and 1.450 Å, respectively) are similar to

Table 3. Selected bond lengths (*d*) in the structure of **3a**

Bond	*d*/Å	Bond	*d*/Å
Cl(1)—C(3)	1.732(6)	Cl(1A)—C(3A)	1.736(5)
C(11)—C(12)	1.447(7)	C(11A)—C(17A)	1.421(7)
N(1)—C(1)	1.338(5)	N(1A)—C(1A)	1.333(5)
C(11)—C(17)	1.455(8)	C(11A)—C(12A)	1.446(7)
N(1)—C(9)	1.366(6)	N(1A)—C(9A)	1.356(6)
C(12)—C(13)	1.535(8)	C(12A)—C(13A)	1.531(8)
O(2)—C(17)	1.239(6)	O(1A)—C(12A)	1.232(6)
C(13)—C(14)	1.461(10)	C(13A)—C(14A)	1.478(9)
O(1)—C(12)	1.240(6)	O(2A)—C(17A)	1.246(6)
C(13)—C(16)	1.575(7)	C(13A)—C(16A)	1.596(7)
C(1)—C(11)	1.384(7)	C(1A)—C(11A)	1.418(7)
C(14)—C(15)	1.406(9)	C(14A)—C(15A)	1.352(9)
C(1)—C(2)	1.451(6)	C(1A)—C(2A)	1.448(6)
C(14)—C(18)	1.425(10)	C(14A)—C(18A)	1.440(8)
C(2)—C(3)	1.321(7)	C(2A)—C(3A)	1.343(7)
C(15)—C(16)	1.440(10)	C(15A)—C(16A)	1.483(9)
C(3)—C(4)	1.439(7)	C(3A)—C(4A)	1.420(7)
C(16)—C(17)	1.552(8)	C(16A)—C(17A)	1.541(8)
C(4)—C(9)	1.411(7)	C(4A)—C(9A)	1.425(7)
C(16)—C(22)	1.625(10)	C(16A)—C(22A)	1.603(9)

those in two compounds containing the analogous 1,3-dioxocyclopentylidene fragment, *viz.*, 2-(1-*N*-phenylaminoethylidene)-indane-1,3-dione[5] and 2-[2(1*H*)-pyridinylidene]-(1*H*)-indene-1,3(2*H*)-dione,[6] whose structures were retrieved from the Cambridge Structural Database (CSD).

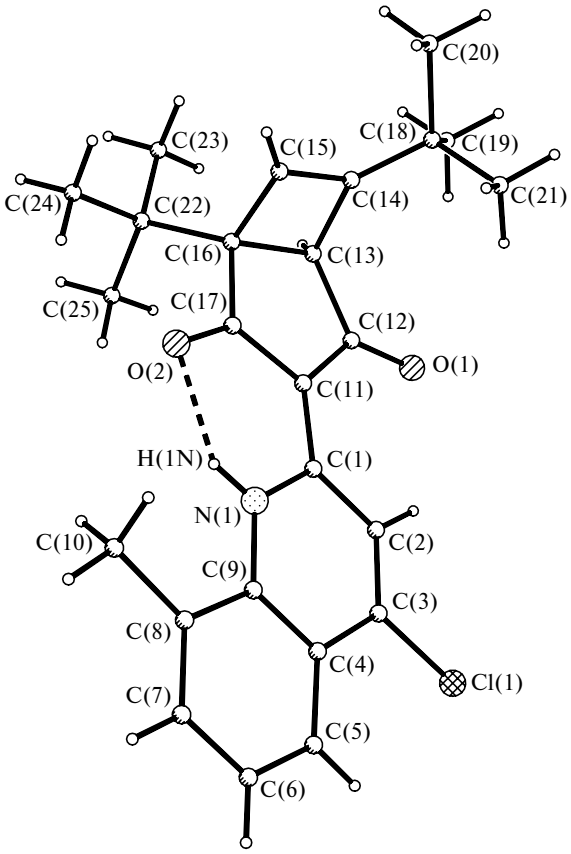

Fig. 3. Overall view of molecule **3a**.

Table 4. Bond angles (ω) in the structure of **3a**

Angle	ω/deg	Angle	ω/deg	Angle	ω/deg
C(1)—N(1)—C(9)	124.5(4)	C(18)—C(14)—C(13)	130.0(7)	C(1A)—C(11A)—C(17A)	121.4(5)
N(1)—C(1)—C(11)	118.2(4)	C(14)—C(15)—C(16)	94.4(6)	C(1A)—C(11A)—C(12A)	126.7(5)
N(1)—C(1)—C(2)	117.4(4)	C(15)—C(16)—C(17)	109.1(7)	C(17A)—C(11A)—C(12A)	111.9(5)
C(11)—C(1)—C(2)	124.1(4)	C(15)—C(16)—C(13)	86.5(5)	O(1A)—C(12A)—C(11A)	128.6(5)
C(3)—C(2)—C(1)	119.5(4)	C(17)—C(16)—C(13)	102.8(5)	O(1A)—C(12A)—C(13A)	123.8(5)
C(2)—C(3)—C(4)	123.0(5)	C(15)—C(16)—C(22)	119.7(5)	C(11A)—C(12A)—C(13A)	107.6(4)
C(2)—C(3)—Cl(1)	119.8(4)	C(17)—C(16)—C(22)	115.7(5)	C(14A)—C(13A)—C(12A)	117.0(7)
C(4)—C(3)—Cl(1)	117.2(4)	C(13)—C(16)—C(22)	118.6(6)	C(14A)—C(13A)—C(16A)	87.1(5)
C(9)—C(4)—C(3)	116.1(5)	O(2)—C(17)—C(11)	124.6(5)	C(12A)—C(13A)—C(16A)	107.0(4)
N(1)—C(9)—C(8)	119.2(5)	O(2)—C(17)—C(16)	124.4(5)	C(15A)—C(14A)—C(18A)	136.8(6)
N(1)—C(9)—C(4)	119.5(4)	C(11)—C(17)—C(16)	111.0(5)	C(15A)—C(14A)—C(13A)	92.7(5)
C(8)—C(9)—C(4)	121.3(5)	C(1A)—N(1A)—C(9A)	124.8(4)	C(18A)—C(14A)—C(13A)	130.4(6)
C(1)—C(11)—C(12)	128.0(5)	N(1A)—C(1A)—C(11A)	118.2(4)	C(14A)—C(15A)—C(16A)	96.7(5)
C(1)—C(11)—C(17)	122.3(4)	N(1A)—C(1A)—C(2A)	117.9(4)	C(15A)—C(16A)—C(17A)	111.9(6)
C(12)—C(11)—C(17)	109.7(5)	C(11A)—C(1A)—C(2A)	123.9(4)	C(15A)—C(16A)—C(13A)	83.4(5)
O(1)—C(12)—C(11)	127.6(5)	C(3A)—C(2A)—C(1A)	118.3(4)	C(17A)—C(16A)—C(13A)	102.2(5)
O(1)—C(12)—C(13)	123.1(4)	C(2A)—C(3A)—C(4A)	123.8(5)	C(15A)—C(16A)—C(22A)	120.1(5)
C(11)—C(12)—C(13)	109.2(5)	C(2A)—C(3A)—Cl(1A)	118.6(4)	C(17A)—C(16A)—C(22A)	115.8(5)
C(14)—C(13)—C(12)	114.3(7)	C(4A)—C(3A)—Cl(1A)	117.6(4)	C(13A)—C(16A)—C(22A)	117.9(6)
C(14)—C(13)—C(16)	86.8(5)	C(3A)—C(4A)—C(9A)	115.7(4)	O(2A)—C(17A)—C(11A)	126.0(5)
C(12)—C(13)—C(16)	107.1(4)	N(1A)—C(9A)—C(4A)	119.5(4)	O(2A)—C(17A)—C(16A)	123.0(5)
C(15)—C(14)—C(18)	137.7(8)	N(1A)—C(9A)—C(8A)	119.4(5)	C(11A)—C(17A)—C(16A)	111.0(4)
C(15)—C(14)—C(13)	92.3(6)	C(4A)—C(9A)—C(8A)	121.1(5)		

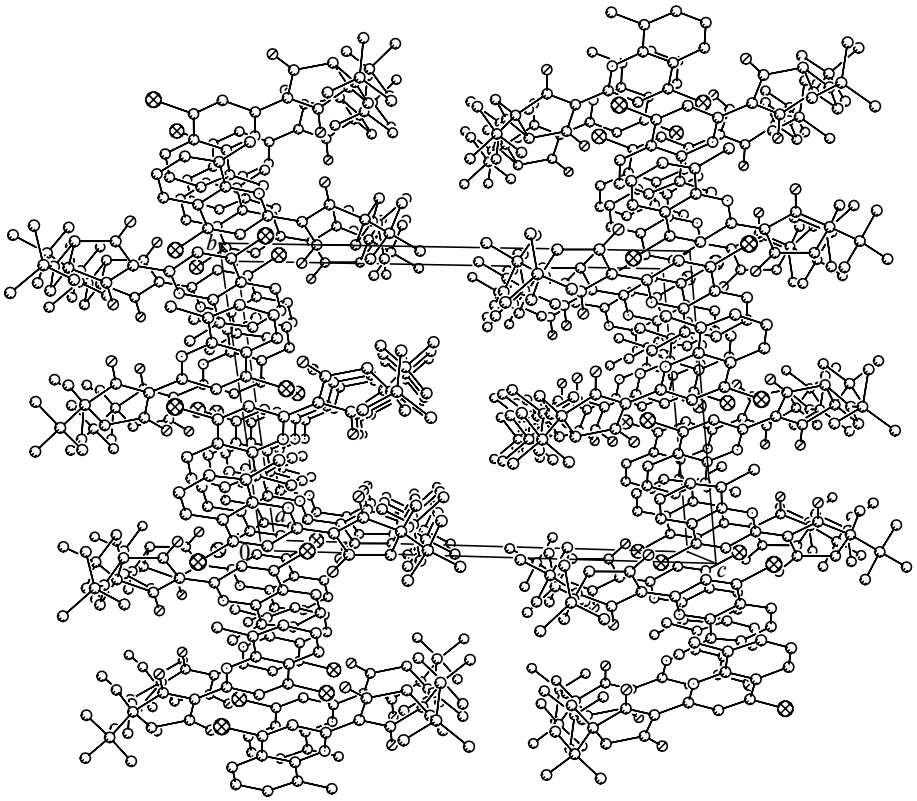

Fig. 4. Stacking interactions between the aromatic fragments in the crystal of **3a**.

In the crystal structure, molecules **3a** are packed in stacks along the *a* axis. In these stacks, the aromatic fragments of both independent molecules are involved in stacking interactions; the distances between the planes of these fragments are 3.37—3.44 Å. The stacks are linked to each other to form layers parallel to the *ab* plane by weak Cl...HC(10) hydrogen bonds (Cl...H, 2.88 and 2.92 Å). The outer surface of the layers is formed by the *tert*-butyl groups (Fig. 4).

The reaction mechanism of photocyclization **1** → **3** presented in Scheme 1 was confirmed by quantum chemical calculations for model compound **1′**. According to the calculations (Table 5), the first step of photoinitiated transformations of **1′** involves the intramolecular proton trans-

Table 5. Total energies (E_{total}/a.u.) and relative energies* (ΔE_{rel}/kcal mol^{-1}) in compounds **1′—3′** and transition states (TS) of the corresponding reactions predicted by the *ab initio* RHF/6-31G(d,p) method in the gas phase and taking into account solvation[7,8]

Compound	Gas			DMSO			Toluene		
	E_{total}	ΔE_{rel}	ΔE_{react}	E_{total}	ΔE_{rel}	ΔE_{react}	E_{total}	ΔE_{rel}	ΔE_{react}
1′	−1587.663702	0.0	0.0	−1587.675674	0.0	0.0	−1587.670334	0.0	0.0
$TS_{\mathbf{1}'-E\text{-}\mathbf{2}'}$	−1587.652165	7.2	7.2	−1587.665673	6.3	6.3	−1587.659630	6.7	6.7
E-**2′**	−1587.661643	1.3	1.3	−1587.677175	−0.9	−0.9	−1587.670185	0.1	0.1
E-**2′**	−1587.661643	1.3	0.0	−1587.677175	−0.9	0.0	−1587.670185	0.1	0.0
$TS_{E\text{-}\mathbf{2}'-Z\text{-}\mathbf{2}'}$	−1587.626231	23.5	22.2	−1587.656761	11.9	12.8	−1587.643046	17.1	17.0
Z-**2′**	−1587.659122	2.9	1.6	−1587.674559	0.7	1.6	−1587.667560	1.7	1.6
Z-**2′**	−1587.659122	2.9	0.0	−1587.674559	0.7	0.0	−1587.667560	1.7	0.0
$TS_{Z\text{-}\mathbf{2}'-Z\text{-}\mathbf{3}'}$	−1587.540737	77.2	74.3						
Z-**3′**	−1587.672047	−5.2	−8.1	−1587.687961	−7.7	−8.4	−1587.680770	−6.6	−8.3
Z-**3′**	−1587.672047	−5.2	0.0	−1587.687961	−7.7	0.0	−1587.680770	−6.6	0.0
$TS_{Z\text{-}\mathbf{3}'-E\text{-}\mathbf{3}'}$	−1587.622752	25.7	30.9	−1587.658452	10.8	18.5	−1587.642521	17.5	24.0
E-**3′**	−1587.671784	−5.1	0.2	−1587.687659	−7.5	0.2	−1587.680506	−6.4	0.2

Note. 1 a.u. = 627.5095 kcal mol^{-1}; ΔE_{react} is the relative energies for the corresponding components of the reactions.
* Compared to the structure of **1′**.

fer **1′** → *E*-**2′**, during which the barrier of 6—7 kcal mol^{-1} is overcome depending on the solvent. As demonstrated above, this process was confirmed by fluorescence studies at 77 K. At room temperature, the rotation about the C—C bond occurs (*E*-**2′** → *Z*-**2′**). The barrier for this reaction is substantially higher (17 kcal mol^{-1} for a nonpolar solvent (toluene) and 12.8 kcal mol^{-1} for a polar solvent (DMSO)). This step of the reaction mechanism was not experimentally documented. However, only cyclization of structure *Z*-**2′** can afford the experimentally observed structure *Z*-**3′**. The calculated reaction barrier for cyclization in the ground state is 70 kcal mol^{-1}, which excludes the possibility of this reaction under thermal conditions.

The geometric parameters of molecule **3′** calculated by the *ab initio* RHF/6-31(d,p) method (Fig. 5) agree well with the experimental data (the discrepancy is ~0.01 Å). At the same time, the calculated geometric parameters of the N—H...O hydrogen bond are somewhat more different from the experimental values (O...H, 1.86 Å; N—HN—O, 136.5°; N...O, 2.68 Å). This fact can be attributed to high mobility of the hydrogen atom and, as a consequence, to a change in its position depending on the solvent.

At room temperature, two geometric isomers of compounds **3**, *E*-**3** and *Z*-**3**, were found in solutions at room temperature, which is manifested in the ^{1}H NMR spectra as doubling of the signals of the *tert*-butyl groups and the vinyl proton of the cyclobutene ring (see Fig. 6). The ratio of the isomers was 40 : 60 (toluene or DMSO). At high temperatures, the exchange process *E*-**3** ⇌ *Z*-**3** was observed by ^{1}H NMR spectroscopy. This process was detected from the dynamics of the signals for the vinyl protons (Fig. 6). The barrier to the rearrangement in DMSO calculated based on the line shape analysis is $\Delta G^{\neq}_{25}$ = 19.1 kcal mol^{-1}.

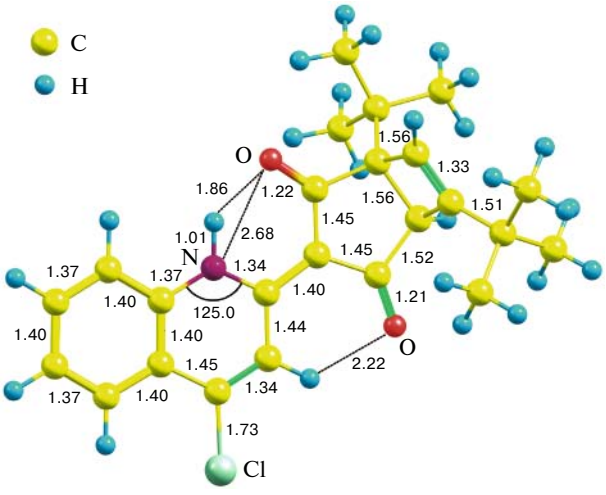

Fig. 5. Geometric characteristics of compound **3′** calculated by the *ab initio* RHF/6-31(d,p) method.

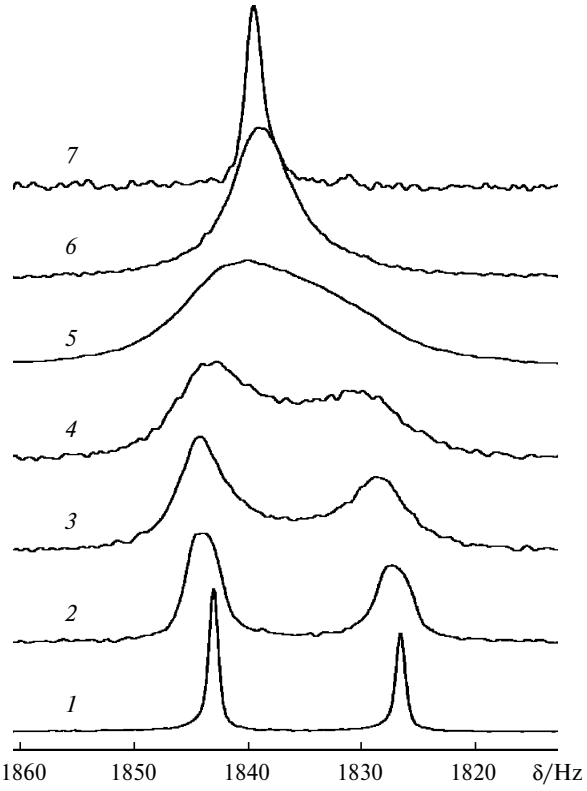

Fig. 6. Temperature evolution of t he signals for the vinyl protons of the bicyclic fragment of compound **3a** in DMSO-d_6, *T*/°C: 40 (*1*), 80 (*2*), 100 (*3*), 110 (*4*), 120 (*5*), 140 (*6*), and 170 (*7*); *k*/s^{-1}: 0.1 (*1*), 5.2 (*2*), 9.4 (*3*), 16.6 (*4*), 35.1 (*5*), 79.9 (*6*), and 451.3 (*7*).

Calculations by the *ab initio* RHF/6-31G(d,p) method taking into account solvation in DMSO accurately reproduced the energy characteristics of the rearrangement *E*-**3** ⇌ *Z*-**3** (Fig. 7). It should be noted that the isomerization barrier calculated without considering the solvating role of the solvent is substantially higher than that determined by dynamic NMR spectroscopy.

Therefore, the experimental and theoretical data allowed us to elucidate the mechanism (see Scheme 1) of the photochemical rearrangement of quinolin-2-yl-substituted β-tropolones **1**. The first step of this mechanism involves the adiabatic proton transfer from the oxygen atom of the tropolone ring to the nitrogen atom of the quinoline fragment in the singlet excited state (**1** ⇌ *E*-**2**) followed by the *cis*-*trans* photoisomerization (*E*-**2** ⇌ *Z*-**2**) typical of compounds with an intramolecular O—H...N hydrogen bond.[9—11] The electrocyclic rearrangement giving a mixture of enantiomers of chiral photoproducts **3** through two possible disrotatory processes is the determining direction of the photochemical reaction.

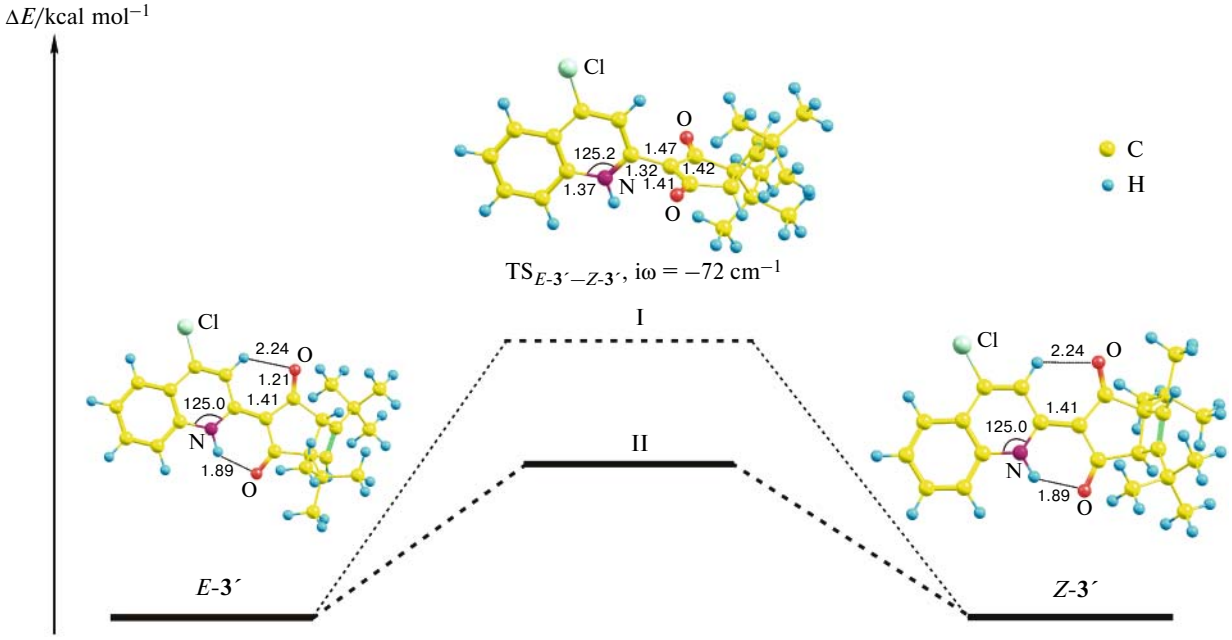

Fig. 7. Reaction energy profile of the rearrangement *E*-**3′** ⇌ *Z*-**3′** based on the results of RHF/6-31G(d,p) calculations; iω is the imaginary frequency for the transition state $TS_{E\text{-}3'—Z\text{-}3'}$ in the gas phase: (I) ΔE = 31 kcal mol^{-1} (the solvent was ignored), and (II) ΔE = 185 kcal mol^{-1} (DMSO).

Experimental

The ^{1}H NMR spectra were recorded on a Varian Unity-300 spectrometer; the chemical shifts are given relative to Me_4Si as the internal standard; $CDCl_3$, $C_6D_5CD_3$, and $(CD_3)_2SO$ were used as the solvents. The kinetic parameters were determined from the broadening of the spectral lines of the indicator protons.[12] The activation parameters were calculated by analyzing the Eyring dependence of ln*k* on 1/*T*. The mass spectra were obtained on a Finnigan MAT INOS 50 mass spectrometer. The electronic absorption spectra were recorded on Specord M-40 and Agilent 8453 spectrophotometers. The photoinduced changes in the electronic absorption spectra were recorded on a diode-matrix Agilent 8453 spectrophotometer with direct irradiation of solutions. The volume of the photolyzed stirred solution in a quartz cell (1×1 cm) was 2 mL. The solutions were irradiated with monochromatic light after passing through a water IR filter and an interference light filter to select the line at 365 nm of the mercury spectrum of a DRSh-250 lamp. The intensity of the incident beam measured with the use of potassium ferrioxalate was 4.06—4.85 • 10^{16} quantum s^{-1}. The quantum yield of the photochemical reaction in the case of the complete overlap of the spectra of the reagent and the reaction product was determined according to a procedure described earlier.[13] Fluorescence measurements were carried out on a Shimadzu RF 5001 PC spectrofluorimeter. The fluorescence quantum yields were determined by the Parker—Rees method[14] with the use of 3-methoxybenzanthrone in toluene (φ = 0.1, λ_{rad} = 365 nm) as the reference luminophore.[15] All calculations were carried out according to the restricted Hartree—Fock method with the split-valence 6-31G(d,p) basis set using the Gaussian 98[16] and GAMESS programs.[17] The stationary points on potential energy surfaces were found by performing full geometry optimization of the molecular structures corresponding to the energy minima and saddle points. The structures corresponding to the energy minima on potential energy surfaces were determined by the steepest descent method (the movement along the gradient line) from the saddle point to the adjacent stationary point.

Compounds **1a—e** were prepared according to a procedure described earlier.[4]

1,6-Di(*tert*-butyl)-3-(4-chloro-8-methyl-1*H*-quinolin-2-ylidene)bicyclo[3.2.0]hept-6-ene-2,4-dione (3a) was synthesized by irradiation of a solution of compound **1a** (50 mg, 0.12 mmol) in hexane (500 mL) in a quartz photoreactor with the use of a DRT-230 mercury lamp for 6 h and with bubbling air through the solution. The course of the reaction was monitored by UV spectroscopy. After completion of irradiation, the solvent was evaporated, and the dry residue was dissolved in a 2 : 1 hexane : benzene mixture and passed through an alumina column (750 • 15 mm) using the same mixture as the eluent. The first fraction contained the unconsumed starting compound **1a**, and the second (intensely fluorescent) fraction contained photoproduct **3a**. The solvent was evaporated and the residue was recrystallized from heptane. A mixture of *E*-**3a** (40%) and *Z*-**3a** (60%) was obtained as yellow crystals in a yield of 32.5 mg (65%), m.p. 223—224 °C. Found (%): C, 73.23; H, 6.74; Cl, 8.67; N, 3.50. $C_{25}H_{28}ClNO_2$. Calculated (%): C, 73.25; H, 6.88; Cl, 8.65; N, 3.42. ^{1}H NMR ($CDCl_3$), δ: 1.08 (s, 18 $H_{E,Z}$, 1.6 Bu^t); 2.71 and 2.74 (both s, 1.2 H_E, 1.8 H_Z, Me(8′)); 3.45 and 3.50 (both s, 0.6 H_Z, 0.4 H_E, H(5)); 6.09 and 6.12 (both s, 0.4 H_E, 0.6 H_Z, H(7)); 7.43 (t, 1 $H_{E,Z}$, H(6′), J = 7.8 Hz); 7.60 (d, 1 $H_{E,Z}$, H(7′), J = 7.8 Hz); 7.99 (d, 1 $H_{E,Z}$, H(5′), J = 7.8 Hz); 8.89 and 8.93 (both s, 0.6 H_Z, 0.4 H_E, H(3′)); 15.63 and 15.70 (both br.s, 0.4 H_E, 0.6 H_Z, NH). ^{1}H NMR (DMSO-d_6), δ: 0.9—1.1 (m, 18 $H_{E,Z}$, 1.6 Bu^t); 2.63 and 2.65 (both s, 1.2 H_E, 1.8 H_Z, Me(8′)); 3.40 and 3.49 (both s, 0.6 H_Z, 0.4 H_E, H(5)); 6.09 and 6.14 (both s, 0.4 H_E, 0.6 H_Z, H(7)); 7.58 (t, 1 $H_{E,Z}$, H(6′), J = 7.8 Hz); 7.82 (d, 1 $H_{E,Z}$, H(7′), J = 7.8 Hz); 7.98

(d, 1 $H_{E,Z}$, H(5′), J = 7.8 Hz); 8.69 and 8.71 (both s, 0.6 H_Z, 0.4 H_E, H(3′)); 15.45 and 15.49 (both br.s, 0.4 H_E, 0.6 H_Z, NH). MS (EI, 70 eV), m/z (I_{rel} (%)): 409.9 $[M]^+$ (65), 353 $[M - Bu^t]^+$ (95), 338 $[M - Bu^t - Me]^+$ (100), 296 $[M - 2\ Bu^t]^+$ (24), 57 $[Bu^t]^+$ (60).

1,6-Di(*tert*-butyl)-3-(4-chloro-6,8-dimethyl-1*H*-quinolin-2-ylidene)bicyclo[3.2.0]hept-6-ene-2,4-dione (3c) was synthesized analogously to compound **3a** in 67% yield. Yellow crystals, m.p. 218—219 °C (from heptane). Found (%): C, 73.57; H, 7.02; Cl, 8.18; N, 3.34. $C_{26}H_{30}ClNO_2$. Calculated (%): C, 73.66; H, 7.13; Cl, 8.36; N, 3.30. ^{1}H NMR ($CDCl_3$), δ: 1.05—1.12 (m, 18 $H_{E,Z}$, 1.6 Bu^t); 2.49 (s, 3 $H_{E,Z}$, Me(6′)); 2.68 and 2.70 (both s, 1.2 H_E, 1.8 H_Z, Me(8′)); 3.44 and 3.49 (both s, 0.6 H_Z, 0.4 H_E, H(5)); 6.09 and 6.13 (both s, 0.4 H_E, 0.6 H_Z, H(7)); 7.43 (s, 1 $H_{E,Z}$, H(7′)); 7.76 (s, 1 $H_{E,Z}$, H(5′)); 8.87 and 8.91 (both s, 0.6 H_Z, 0.4 H_E, H(3′)); 15.66 and 15.72 (both br.s, 0.4 H_E, 0.6 H_Z, NH).

X-ray diffraction study of compound **3a**. X-ray diffraction data (12861 reflections) were collected on a Bruker SMART CCD diffractometer at 120 K (λ(Mo-K_α) radiation, $2\theta_{max} = 50°$) from a single crystal of dimensions 0.35×0.30×0.15 mm. After merging of the equivalent reflections, the data sets consisted of 7252 independent reflections (R_{int} = 0.0923), which were used for the structure solution and refinement. Absorption (μ = 0.197 mm^{-1}) was ignored. Yellow plate-like crystals of **3a**, $C_{25}H_{28}ClNO_2$, M = 409.95, are triclinic. At 120 K a = 10.202(4) Å, b = 12.589(6) Å, c = 17.981(8) Å, α = 95.738(9)°, β = 96.849(9)°, γ = 107.222(9)°, V = 2168(2) $Å^3$, space group $P\bar{1}$, Z = 4, d_{calc} = 1.256 g cm^{-3}. The structure was solved by direct methods. Nonhydrogen atoms were located in difference electron density maps and refined against F^2_{hkl} with anisotropic displacement parameters. All hydrogen atoms were placed in geometrically calculated positions and refined using a riding model with $U(H) = n\ U(C)$, where $U(C)$ is the equivalent thermal parameter of the pivot carbon atom, n = 1.2 and 1.5 for the sp^2- and sp^3-hybridized carbon atoms, respectively. The final R factors were R_1 = 0.0946 (calculated against F_{hkl} for 3175 reflections with $I > 2\sigma(I)$), wR_2 = 0.1898 (calculated against F^2_{hkl} for all 7252 reflections), and GOOF = 0.983; 523 parameters were refined. All calculations were performed with the use of the SHELXTL PLUS 5 program package.[18] The atomic coordinates and atomic displacement parameters were deposited with the Cambridge Structural Database (CCDC 291792).

This study was financially supported by the Russian Foundation for Basic Research (Project No. 05-03-32081-a), the Council on Grants of the President of the Russian Federation (Program for State Support of Leading Scientific Schools of the Russian Federation (Grant NSh-945.2003.3), and the International Foundation "Scientific Partnership."

References

1. W. G. Dauben, K. Koch, S. L. Smith, and O. L. Chapman, *J. Am. Chem. Soc.*, 1963, **85**, 2616.
2. L. S. Kaanumalle, J. Sivaguru, N. Arunkumar, S. Karthikeyan, and V. Ramamurthy, *Chem. Commun.*, 2003, 116.
3. J. Sivaguru, A. Natarajan, L. S. Kaanumalle, J. Shailaja, S. Uppili, A. Joy, and V. Ramamurthy, *Acc. Chem. Res.*, 2003, **36**, 509.
4. V. N. Komissarov, D. N. Bang, V. I. Minkin, S. M. Aldoshin, V. V. Tkachev, and G. V. Shilov, *Mendeleev Commun.*, 2003, 219.
5. V. Enchev, G. Ivanova, G. Pavlovic, M. Rogojerov, A. Ahmedova, and M. Mitewa, *J. Mol. Struct.*, 2003, **654**, 11.
6. A. A. Kemme, M. F. Bundule, Ya. Ya. Bleidelis, E. E. Liepin´sh, E. S. Lavrinovich, and Yu. E. Fridmanis, *Khim. Geterotsikl. Soedin.*, 1978, 1076 [*Chem. Heterocycl. Compd.*, 1978, 865 (Engl. Transl.)].
7. H. Li, C. S. Pomelli, and J. H. Jensen, *Theoret. Chim. Acta*, 2003, **109**, 71.
8. J. Tomasi and M. Persico, *Chem. Rev.*, 1994, **94**, 2027.
9. S. G. Formosinho and L. G. Arnaud, *J. Photochem. Photobiol. A: Chem.*, 1994, **75**, 21.
10. M. I. Knyazhanskii and A. V. Metelitsa, *Fotoinitsiirovannye protsessy v molekulakh azometinov i ikh strukturnykh analogov* [*Photoinduced Processes in Azomethine Molecules and Their Structural Analogs*], Izd-vo Rost. Un-ta, Rostov-on-Don, 1992, p. 77 (in Russian).
11. M. I. Knyazhanskii, N. I. Makarova, E. P. Olekhnovich, V. A. Pichko, and V. A. Kharlanov, *Zh. Org. Khim.*, 1996, **32**, 1097 [*Russ. J. Org. Chem.*, 1996, **32**, 1059 (Engl. Transl.)].
12. B. I. Ionin, B. A. Ershov, and A. I. Kol´tsov, *YaMR-spektroskopiya v organicheskoi khimii* [*NMR Spectroscopy in Organic Chemistry*], Khimiya, Leningrad, 1983, p. 254 (in Russian).
13. *Eksperimental´nye metody khimicheskoi kinetiki* [*Experimental Methods of Chemical Kinetics*], Eds N. M. Emmanuel' and M. G. Kuz´min, Izd-vo MGU, Moscow, 1985, p. 266 (in Russian).
14. C. A. Parker, *Photoluminescence of Solutions. With Applications to Photochemistry and Analytical Chemistry*, Elsevier Publishing Company, Amsterdam—London—New York, 1968.
15. B. M. Krasovitskii and B. M. Bolotin, *Organicheskie lyuminofory* [*Organic Luminophores*], Khimiya, Moscow, 1984, p. 292 (in Russian).
16. M. J. Frisch, G. W. Trucks, H. B. Schlegel, G. E. Scuseria, M. A. Robb, J. R. Cheeseman, V. G. Zakrzewski, J. A. Montgomery, Jr., R. E. Stratmann, J. C. Burant, S. Dapprich, J. M. Millam, A. D. Daniels, K. N. Kudin, M. C. Strain, O. Farkas, J. Tomasi, V. Barone, M. Cossi, R. Cammi, B. Mennucci, C. Pomelli, C. Adamo, S. Clifford, J. Ochterski, G. A. Petersson, P. Y. Ayala, Q. Cui, K. Morokuma, D. K. Malick, A. D. Rabuck, K. Raghavachari, J. B. Foresman, J. Cioslowski, J. V. Ortiz, A. G. Baboul, B. B. Stefanov, G. Liu, A. Liashenko, P. Piskorz, I. Komaromi, R. Gomperts, R. L. Martin, D. J. Fox, T. Keith, M. A. Al-Laham, C. Y. Peng, A. Nanayakkara, M. Challacombe, P. M. W. Gill, B. Johnson, W. Chen, M. W. Wong, J. L. Andres, C. Gonzalez, M. Head-Gordon, E. S. Replogle, and J. A. Pople, *Gaussian 98, Revision A.9*, Gaussian, Inc., Pittsburgh PA, 1998.
17. M. W. Schmidt, K. K. Baldridge, J. A. Boatz, S. T. Elbert, M. S. Gordon, J. J. Jensen, S. Koseki, N. Matsunaga, K. A. Nguyen, S. Su, T. L. Windus, M. Dupuis, and J. A. Montgomery, *J. Comput. Chem.*, 1993, **14,** 1347.
18. G. M. Sheldrick, *SHELXTL v. 5.10*, *Structure Determination Software Suite*, Bruker AXS, Madison, Wisconsin, USA, 1998.

Received September 3, 2005;
in revised form December 12, 2005